Noise in three-dimensional nanowires

A. G. Scherbakov, E. N. Bogachek, and Uzi Landman
School of Physics, Georgia Institute of Technology, Atlanta, Georgia 30332-0430
(Received 27 October 1997)

Noise spectra in adiabatically shaped three-dimensional nanowires, modeled via hard- and soft-wall confining potentials, are studied in field-free conditions and under the influence of applied magnetic fields, as well as finite voltages. Quantum-shot-noise peaks in such nanowires occur when the quantized conductance of the wire changes from one conductance plateau to another. The amplitudes of these peaks are suppressed for effectively longer wires reflecting enhancement of the time correlation between current-carrying states. In a magnetic field the shot-noise peaks split and shift due to lifting of degeneracies and shifting of the energies of the conducting modes. This can lead to magnetic-field-induced blockade of shot noise in nanowires. In a transverse magnetic field cross-sectional shape anisotropy of the nanowire may influence the noise spectrum due to dependence of the contributions from current-carrying edge states on the direction of the applied field. Control of the noise spectrum in nanowires through applied finite voltages in field-free conditions and under the influence of applied magnetic fields is demonstrated. [S0163-1829(98)05211-4]

I. INTRODUCTION

Ballistic quantum systems are unique objects where electronic quantum properties may be manifested on a macroscopic level. One of the most intriguing examples of such systems is a ballistic nanoconstriction, or a nanowire. Due to the discrete character of the electronic spectrum, transport through such nanowires is characterized by kinetic coefficients exhibiting new features, such as conductance quantization in units of $2e^2/h$ and thermopower peaks as a function of the electron energy (or equivalently, the physical dimension of the nanowire), which differ from their classical counterparts. Such behavior occurs in two-dimensional (2D) wires[1] as well as in three-dimensional (3D) ones.[2–4]

In this paper we focus on investigations of noise in 3D nanowires. Two sources of noise occurring in ballistic systems have been identified: (i) thermal or Johnson-Nyquist noise and (ii) shot noise (see, for example, reviews in Refs. 5 and 6). The latter is due to discreteness of the charges of the electrons and occurs only under appropriate conditions. Early investigations[7] demonstrated the absence of shot noise in classical ballistic constrictions (with sizes much greater than the Fermi wavelength, λ_F) where the conductance can be described by the Sharvin expression.[8]

The situation may change significantly in constrictions with lateral sizes comparable to λ_F. In such systems quantum electronic transport can be described in the framework of a Landauer, or scattering, formalism.[9] Application of this approach to studies of noise properties[10–13] led to the discovery of the shot noise in 2D quantum constrictions.[11–14] It has been shown that noise in quantum point contacts (occurring in the regions of the transitions between conductance plateaus) is suppressed compared to its classical value ($2eI$, where I is the average current and e the electron charge), attaining the full value only in ballistic conductors where the transmission probabilities of all channels are small; this originates from correlations due to the Fermi statistics of the electrons. (Similarly, for a biased quantum conductor at low temperature the probability distribution function of the number of electrons passing through the circuit is binomial rather than Poissonian as is the case for classical shot noise produced by uncorrelated electrons.[5]) Consequently, any factor that decreases the transmission probability of the electron through the nanoconstriction will increase the value of the shot noise in a quantum ballistic conductor; for example, when the length of the quantum wire is shortened or when the electrons have to pass through a tunnel barrier or surmount a high ($\gg k_BT$) barrier.

In this paper we discuss noise properties of 3D nanowires modeled by hard or soft confining potentials. Since common methods for preparation of 3D nanowires[4] (e.g., tip-based methods, mechanical break junctions, and pin-plate setups) do not allow generation of well-controlled reproducible structures, transport in 3D nanowires may be better controlled and studied through the use of applied external fields. To this aim, we demonstrate that shot noise in nanowires may be induced and controlled by applied magnetic fields as well as applied finite voltages.

The paper is organized as follows: (i) in Sec. II we review briefly some of the pertinent aspects of quantum shot noise and outline the method of calculation; (ii) results for noise spectra in 3D nanowires modeled using hard- or soft-wall confining potentials, with and without applied external magnetic fields, are presented in Sec. III, and dependencies on magnetic-field strength and orientation, as well as on the wire's geometry, voltage difference, and temperature, are investigated. A summary of the results is given in Sec. IV.

II. NOISE SPECTRUM AND METHODS OF CALCULATIONS

A. Thermal and quantum shot noise

We consider noise properties of nanowires connecting two reservoirs with a bias voltage applied between them (i.e., $-V/2$ in the upper one and $V/2$ in the lower one, see inset in Fig. 1). In the Landauer formalism the spectral density of the noise, P, may be expressed in terms of the transmission probabilities and in the low-frequency limit it has the form[5,6]

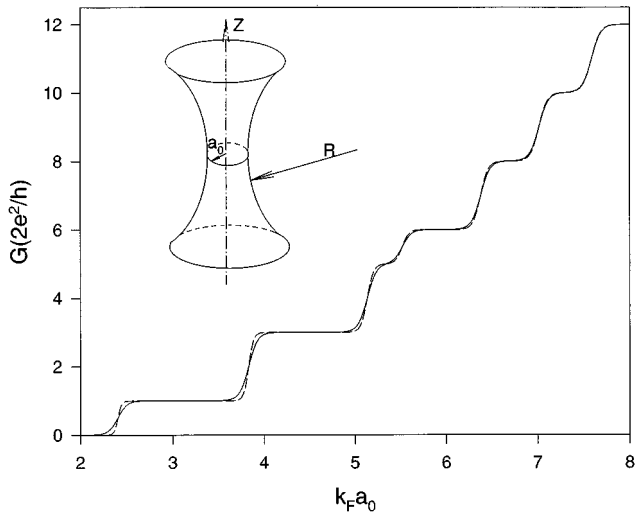

FIG. 1. The conductance (in units of $2e^2/h$) plotted vs $k_F a_0$ for cylindrical wires modeled via a hard-wall confining potential at $T=0$ and for $V\to 0$ and $H=0$. The dashed and solid lines corresponds to constant volume and constant shape elongations of the wire. Note increased smearing of the conductance steps for the constant shape case, particularly as the minimal cross-sectional radius decreases. The geometry of the wire is shown as an inset.

$$P=2\frac{2e^2}{h}\int_o^\infty dE\Big\{[f_1(1-f_2)+f_2(1-f_1)]\sum_\alpha T_\alpha(1-T_\alpha) +[f_1(1-f_1)+f_2(1-f_2)]\sum_\alpha T_\alpha^2\Big\}, \tag{1}$$

here $f_1(E)=f(E-eV/2-\mu)$, $f_2(E)=f(E+\mathrm{eV}/2-\mu)$, f is the Fermi distribution function, and μ is the chemical potential. The transmission probabilities T_α (α denotes the transverse quantum numbers of the electronic states, i.e., conductance channels) are determined from the solution of the Schrödinger equation. We assumed that all the coefficients T_α are of diagonal form (no mode mixing), valid for wires with adiabatically varying shapes.[15]

In equilibrium, for zero applied voltage, Eq. (1) leads to the standard expression for thermal noise

$$P_T=4k_BTG, \tag{2}$$

where G is the conductance of the wire, T is the temperature, and k_B is the Boltzmann constant. In the opposite case of a finite voltage and in the limit of low temperature ($k_BT\ll \mathrm{eV}\ll\mu$, allowing us to neglect any voltage dependence of the transmission coefficients) we have the expression for the shot noise

$$P_V=2\ \mathrm{eV}\frac{2e^2}{h}\sum_\alpha T_\alpha(1-T_\alpha). \tag{3}$$

The latter expression describes peaks of noise spectral density in the vicinities of the conductance steps in 3D wires as well as in 2D ones.[11–14] In the limit $T_\alpha\ll 1$ the shot noise is described by its classical value $P_v=2eI$, where $I=GV$.

For adiabatically varying wires, the transmission probabilities have a Fermi-function-like form (see below),

$$T_\alpha=\frac{1}{1+e^{-\Gamma_\alpha(E-E_\alpha)}}, \tag{4}$$

where Γ_α is a parameter determined by the shape of the wire, and in general it depends also on the conducting channel. As shown below [see Eq. (15)] the parameter Γ_α for a wire modeled via a soft-wall confining potential is independent of the conducting channel, i.e., $\Gamma_\alpha=\Gamma$ for all α. Consequently, in this model $T_\alpha(1-T_\alpha)=(1/\Gamma)\partial T_\alpha/\partial E$, and taking into account the definition of the conductance we obtain

$$P_V=\frac{2\ \mathrm{eV}}{\Gamma}\frac{\partial G}{\partial\mu}. \tag{5}$$

From the expression for the thermopower coefficient of the nanowire (see, for example, Ref. 16)

$$S=\frac{\pi^2k_B^2T}{3e}\frac{\sum_\alpha \frac{\partial T_\alpha}{\partial E}}{\sum_\alpha T_\alpha}, \tag{6}$$

it follows that for (adiabatically shaped) wires modeled via a soft-wall model potential the shot-noise power can be expressed as a product of the conductance and thermopower coefficient,

$$P_V=\frac{2V}{TL_0\Gamma}GS, \tag{7}$$

where $L_0=\pi^2k_B^2/3e^2$ is the Lorentz number.

Finally, we comment on the influence of the length of the nanowire on the shot-noise power. For $k_BT\ll\mathrm{eV}$ Eq. (1) reduces to

$$P_V=2\frac{2e^2}{h}\sum_\alpha\frac{1}{\Gamma_\alpha}\left[T_\alpha\left(\mu+\frac{\mathrm{eV}}{2}\right)-T_\alpha\left(\mu-\frac{\mathrm{eV}}{2}\right)\right], \tag{8}$$

with T_α and Γ_α defined in Eq. (4). We will assume that eV is smaller than the spacing between the transverse energy levels. In this case the shot noise (8) as a function of μ (or, equivalently, as a function of the minimum cross-sectional radius a_0), contains a set of peaks located at $\mu=E_\alpha$ (in a plot of the conductance versus μ these points correspond to the centers of the step rises) with their widths equal to eV. Let us consider the maximal value of the shot noise for one of these peaks. For $\mu=E_\alpha$ we obtain

$$P_{V,\max}^\alpha=2\frac{2e^2}{h}\frac{1}{\Gamma_\alpha}\tanh\left(\Gamma_\alpha\frac{\mathrm{eV}}{4}\right). \tag{9}$$

In the limiting case where the parameter $\Gamma_\alpha\ \mathrm{eV}/2\ll 1$, Eq. (9) becomes

$$P_{V,\max}^\alpha=2\ \mathrm{eV}\frac{2e^2}{h}\frac{1}{4}\left[1-\frac{1}{12}\left(\Gamma_\alpha\frac{\mathrm{eV}}{2}\right)^2\right]. \tag{10}$$

Note, that to a linear approximation in V, Eq. (10) yields the same result for the maximal value of the shot noise for channel α (i.e., $T_\alpha=\frac{1}{2}$) as Eq. (3). This sets the condition for the validity of Eq. (3), i.e., $\Gamma_\alpha\ \mathrm{eV}/2\ll 1$. In this context we re-

mark that the generalization of Eq. (3) to include nonlinear corrections to the shot noise can be easily obtained, yielding

$$P_V^{\alpha}=2\ \mathrm{eV}\,\frac{2e^2}{h}\,\frac{\gamma_\alpha}{(1+\gamma_\alpha)^2}\left[1+\frac{1-4\gamma_\alpha+\gamma_\alpha^2}{6(1+\gamma_\alpha)^2}\left(\Gamma_\alpha\,\frac{\mathrm{eV}}{2}\right)^2\right], \tag{11}$$

where $\gamma_\alpha=\exp[\Gamma_\alpha(\mu-E_\alpha)]$.

When $\Gamma_\alpha\ \mathrm{eV}/2>1$, we obtain

$$P_{V,\max}^{\alpha}\simeq 2\,\frac{2e^2}{h}\,\frac{1}{\Gamma_\alpha}. \tag{12}$$

In this limit the maximum value of the shot-noise power is independent of the applied voltage.

It can be easily shown[17,18] that $\Gamma_\alpha\sim\sqrt{R}$, where R is the axial radius of curvature of the nanowire (see inset in Fig. 1). From Eqs. (9)–(12) it follows that the maximum value of the shot noise decreases with an increase of R. This is a manifestation of the enhancement of the time-correlations between current-carrying states in long quantum constrictions (discussed in Ref. 19 in connection with 2D constrictions).

B. Method of calculations

For calculations of the noise spectral density in 3D nanowires we use Eq. (1), with the constrictions modeled by using either hard- or soft-wall confining potentials. In the hard-wall model we assume that the cross sections of the constriction normal to the axis of the wire are circles of radii $a(z)$, with the one in the narrowmost part of the constriction denoted by $a_0\equiv a(0)$ (see inset to Fig. 1). The applied magnetic field is oriented parallel to the axis of the wire (z direction). The transmission probabilities T_α are determined from the solutions of the Schrödinger equation with a Dirichlet boundary condition (i.e., vanishing of the wave function on the surface of the wire). Smoothness of the function $a(z)$ on the scale of k_F^{-1} (k_F is the Fermi wave vector) allows us to use the adiabatic method of separation of variables,[15,2] and the coefficients T_α have a diagonal form (no mode mixing),[17]

$$T_{mn;mn}^{-1}=1+\exp\{-2\pi[E-E_{mn}(0)]/[(-\hbar^2/m^*)\times E''_{mn}(0)]^{1/2}\}, \tag{13}$$

where $E''_{mn}(0)\equiv\partial^2E_{mn}(0)/\partial z^2$, $E_{mn}(z)$ are the adiabatic (transverse) energy levels of electrons for a cross section of radius $a(z)$, m and n are the azimuthal and radial quantum numbers, respectively ($m=0,\pm1,\ldots$; $n=1,2,\ldots$), and m^* is the electronic effective mass. When $H=0$ the energy levels are determined by the zeros of the Bessel function, and for $H\neq0$, they are computed as the zeros of the confluent hypergeometric function.[17] The second derivative of the energy may be expressed in the form[18] $E''_{mn}(0)=-E_{mn}(0)S''(0)/S(0)$, where $S(z)$ is the area of the cross section of the wire at z. In this case the transmission probability is defined in terms of the electronic energy levels at the narrowmost part $E_{mn}(0)$ and the geometrical factor $S''(0)/S(0)$ which determines the effective length of the wire.[18]

In the soft-wall confining potential model we use a 3D generalization[20] of the 2D Buttiker model,[21] which has a form

$$U(x,y,z)=U_0-\tfrac{1}{2}m^*\omega_z^2z^2+\tfrac{1}{2}m^*(\omega_x^2x^2+\omega_y^2y^2). \tag{14}$$

The parameter ω_x/ω_y describes the degree of anisotropy of the cross section of the constriction (being circular when $\omega_x/\omega_y=1$), and the ratio of the effective frequencies ω_x and ω_y to ω_z determines the effective length of the wire.[20] In this model the transmission coefficients may be determined for magnetic fields of arbitrary strengths and directions, and have a form[20] similar to that given in Eq. (13), i.e.,

$$T_{mn;mn}^{-1}=1+\exp\{-2\pi[E-E_{mn}(0)-U_0]/\hbar\omega_z\}. \tag{15}$$

III. QUANTUM NOISE IN 3D NANOWIRES

In this section we present results for quantum noise spectra in 3D nanowires modeled by hard (Sec. III A) or soft (Sec. III B) confining potentials.

A. Hard-wall confining potential

Prior to discussion of the noise spectra we show in Fig. 1 the calculated magnetic-field-free conductance in 3D nanowires with axial cylindrical symmetry (see inset in Fig. 1), for zero temperature and $V\to0$. Results for G (in units of $g_0=2e^2/h$) as a function of k_Fa_0 are shown for two cases: (i) Results calculated for a wire where the ratio R/a_0 between the axial radius of curvature (R) and a_0 is kept constant (i.e., wires of similar shapes) are indicated by a solid line showing a quantization sequence $1g_0,2g_0,2g_0,1g_0,\ldots$ reflecting the cylindrical symmetry of the wire (m degeneracy of the energy levels),[2] with some smearing of the step rises due to tunneling (these corrections decrease for larger values of R/a_0); (ii) since in common methods for generation of nanowires[3,4] they are formed through elongation of a contact with constant volume (as predicted by early molecular-dynamics simulations[3]) we show for comparison results (indicated by a dashed line) for a wire whose volume was kept constant with a value corresponding to $R/a_0=10$ at $k_Fa_0=8$ (in this calculation the radius of the largest cross section was taken as $5a_0$ and held constant, i.e., this calculation simulates stretching and consequent narrowing of the wire, at constant volume). We note diminished smearing of the conductance steps for effectively longer wires (i.e., lower values of k_Fa_0) due to reduced tunneling effects. Apart from somewhat less smearing of the conductance steps for the constant volume case, the results of the above two models are rather similar.

In Fig. 2 we show results for the noise (P in units of $(4e^2/h)E_F$, where E_F is the Fermi energy) for the two models (i.e., constant shape and constant volume elongations, solid and dashed lines, respectively) with $H=0$ and $\mathrm{eV}/E_F=0.05$, for wires with various effective lengths (longer wires correspond to larger values of R/a_0), at a temperature $k_BT/E_F=0.005$ (and for $R/a_0=10$ also for a lower temperature $k_BT/E_F=0.002$, upper curves). The noise on the plateaus is of thermal origin and the peaks at the step rises are mainly due to quantum shot noise. We observe that the amplitude of the shot noise reduces for effectively longer wires (increasing R/a_0), and it is somewhat smaller for the constant volume case. We also note the relative increased shot-noise amplitudes for the lower temperature (compare the two

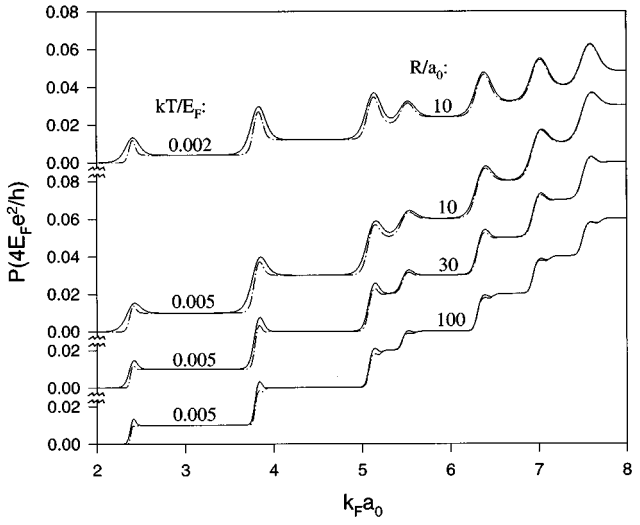

FIG. 2. Noise (in units of $4E_Fe^2/h$) plotted vs k_Fa_0 for cylindrical wires modeled via a hard-wall confining potential; dashed and solid lines correspond to constant volume and constant shape elongations, respectively. In all cases the applied voltage is $eV/E_F=0.05$ and $H=0$. The values of the effective length of the wires (R/a_0) and temperature (k_BT/E_F) are as denoted. Note the reduced shot-noise amplitudes (peaks) for longer wires.

upper sets of curves for $k_BT/E_F=0.005$ and 0.002), due to a decrease in the magnitude of the thermal noise. Since again the results of the two models are rather similar, we limit ourselves in the following to wires elongated with constant shape.

The influence of externally applied longitudinal magnetic fields on the noise spectrum is shown in Fig. 3 for a constant-shape wire ($R/a_0=10$), with $k_BT/E_F=0.005$ and $eV/E_F=0.05$, for two magnetic-field strengths $\hbar\omega_c/E_F=0.15$ and 0.3, where ω_c is the cyclotron frequency $\omega_c=eH/m^*c$. The

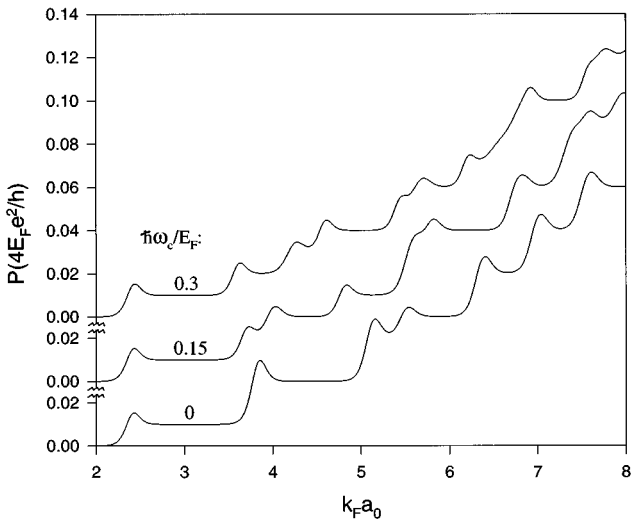

FIG. 3. Noise (in units of $4E_Fe^2/h$) plotted vs k_Fa_0 for a cylindrical wire modeled via a hard-wall confining potential, with $R/a_0=10$, $k_BT/E_F=0.005$, $eV/E_F=0.05$, and for three values of an applied longitudinal magnetic field, specified by $\hbar\omega_c/E_F$ where ω_c is the cyclotron frequency. Note splitting and shifting of (shot) noise peaks induced by the magnetic field.

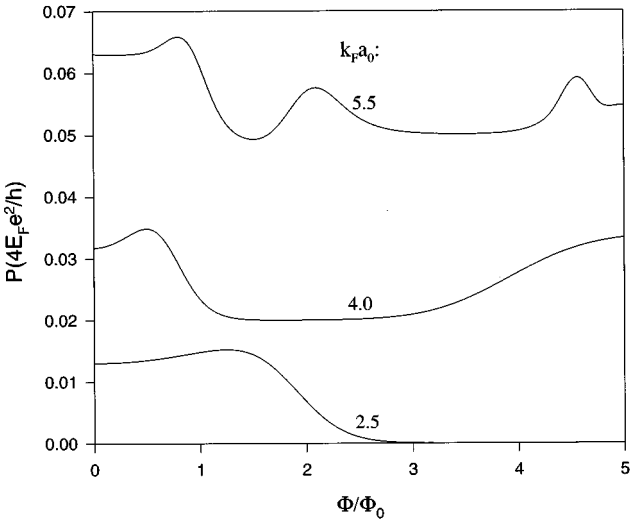

FIG. 4. Noise (in units of $4E_Fe^2/h$) plotted vs φ/φ_0, where $\varphi=\pi a_0^2H$ and $\varphi_0=hc/e$ is the flux quantum, for a cylindrical wire with $R/a_0=10$, $k_BT/E_F=0.005$, and $eV/E_F=0.05$. Results are shown for several configurations of the wire specified by $k_Fa_0=2.5$, 4.0, and 5.5 (corresponding to 1, 3, and 5 conducting channels under magnetic-field free conditions; compare Fig. 1). Note the magnetic-field-induced ''noise blockade,'' for the $k_Fa_0=2.5$ case.

main effect of the magnetic field is to remove the conductance mode degeneracies and shift their energies.[17] This is portrayed by splitting and shifting of the quantum-shot-noise peaks; these effects are progressively more pronounced as H increases.

The noise spectra plotted in Fig. 4 versus φ/φ_0, where $\varphi=\pi a_0^2H$ is the magnetic flux through the narrowest cross section and $\varphi_0=hc/e$ is the flux quantum, for several individual values of k_Fa_0 (2.5, 4.0, and 5.5, corresponding to 1, 3, and 5 conducting channels for $H=0$, see Fig. 1), illustrate the possibility of controlling the amplitude of the noise by the magnetic field, and even achieving ''noise blockade'' for

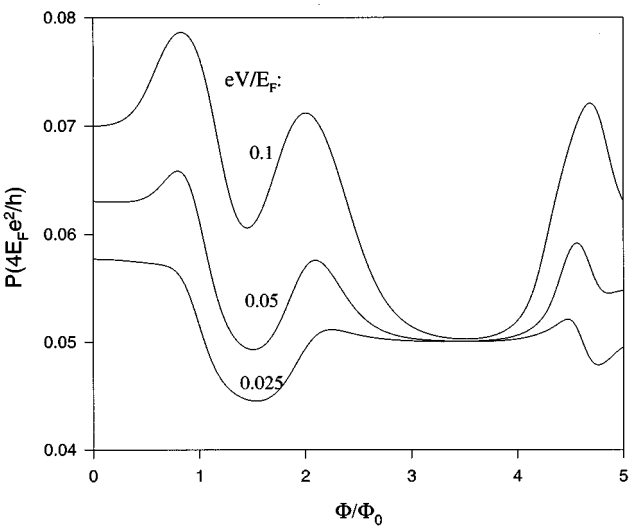

FIG. 5. Dependence of the noise spectrum vs φ/φ_0 shown in Fig. 4 for $k_Fa_0=5.5$, on the magnitude of the applied voltage difference across the wire.

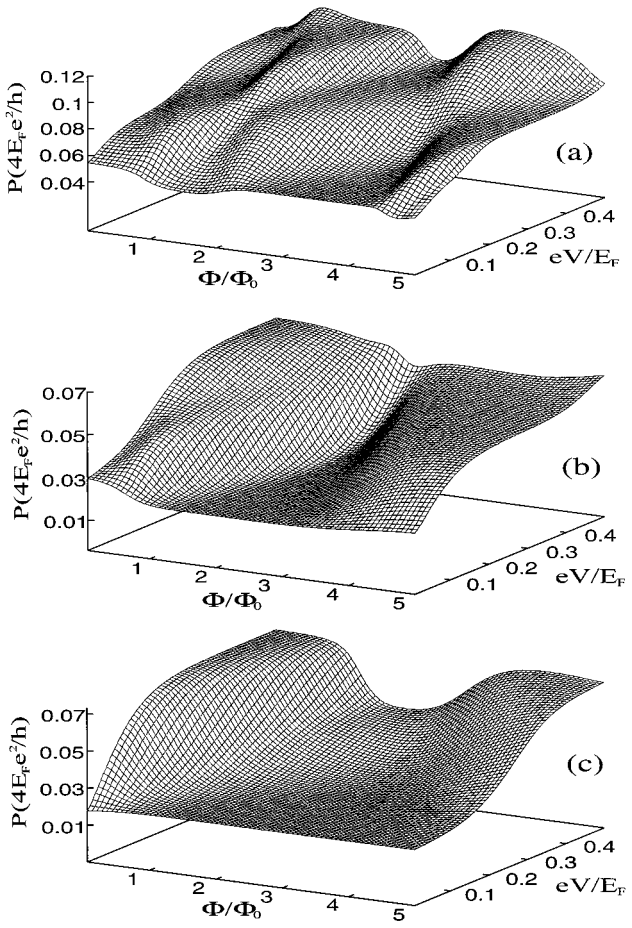

FIG. 6. The noise spectra (in units of $4E_Fe^2/h$) for a hard-wall modeled nanowire with $R/a_0=10$ and $k_BT/E_F=0.005$, plotted, in (a), (b), and (c) for $k_Fa_0=5.5$, 4.0, and 3.8, vs the combined effects of an applied magnetic longitudinal field (φ/φ_0) and voltage difference (eV/E_F).

wires with a small number of conducting channels (see, e.g., $k_Fa_0=2.5$). In comparing the noise spectra versus k_Fa_0 (Fig. 3) with those plotted versus the magnetic field (Fig. 4) we note that for the same wire geometry smearing of the magnetic-field-induced noise peaks is somewhat larger (a similar effect occurs for the conductance of nanowires in a magnetic field[17]). Focusing on the noise spectrum for $k_Fa_0=5.5$ we show in Fig. 5 the influence of the applied magnetic field for several values of the voltage difference across the wires, illustrating increased noise variations for larger V. The combined effects of external magnetic field and voltage are shown in Figs. 6(a)–6(c) for $k_Fa_0=5.5$, 4.0, and 3.8, illustrating the sensitivity of the noise spectrum to these externally applied fields and the level of control that may be achieved through them.

The noise power at finite temperature and voltage incorporates thermal [Eq. (2)] and shot-[Eq. (3)] noise contributions in a nonlinear way. The ''nonadditivity'' of the two sources of noise is illustrated in Fig. 7 where we plotted $\Delta(V,T)=P(V,T)-P(0,T)-P(V,0)$ versus the temperature and the applied voltage for $k_Fa_0=5.5$ and no external magnetic field. From this figure we observe that the noise power at finite voltage and temperature can be bigger or smaller

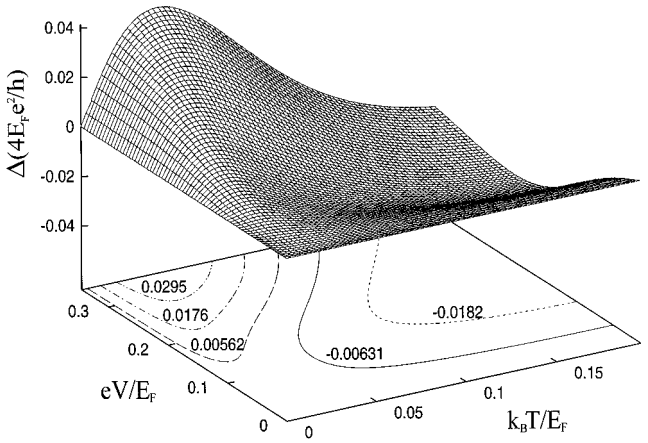

FIG. 7. $\Delta(V,T)=P(V,T)-P(0,T)-P(V,0)$, in units of $4E_Fe^2/h$, plotted vs eV/E_F and k_BT/E_F, for a nanowire modeled by a hard-wall confining potential, with $k_Fa_0=5.5$, and $H=0$. The plot illustrates nonadditivity of the thermal and shot-noise contributions. Contours of $\Delta(V,T)$ are plotted in the voltage-temperature plane, with the corresponding values of Δ as marked.

than the sum of the thermal and shot noise [i.e., $\Delta(V,T)$ can take positive or negative values depending on V and T].

B. Soft-wall confining potential

In the previous section we discussed conductance and quantum shot noise in nanowires modeled by a hard-wall confining potential. In this section we turn to nanowires modeled by a soft-wall confining potential (a generalization of the saddle potential[21] to three-dimensions[20]) which allows analytic solutions, and in particular is convenient for investigations of the effects of the orientation of the applied magnetic field (e.g., longitudinal field along the axis of the wire, or a transverse field along a direction normal to the wire's axis).

As discussed in Sec. II the soft-wall confinement is characterized by quadratic potentials with ω_x and ω_y corresponding to the transverse plane ($\omega_x=\omega_y\equiv\omega_0$ giving a circular cross section), and ω_z describing the axial curvature of the wire. The conductance of wires with such soft-wall confinement is characterized by a higher degree of degeneracy of the (transverse) conductance channels, compared to the corresponding hard-wall confinement, and it is shown in the inset in Fig. 8 for $T=0$, $H=0$, and $V\to0$, plotted versus $\xi=2(E_F-U_0)/\hbar\omega_0$, which is analogous to k_Fa_0 for the hard-wall confinement.

Since for $H=0$ and for a longitudinal magnetic field the features of the noise spectrum are similar to those shown in Sec. III A we focus here on the influence of applied transverse magnetic fields (the method of solution follows closely that described in our earlier study[20]). The noise spectra shown in Fig. 8 for a circular cross-sectional wire for different values of the magnetic-field strength, and for $k_BT/E_F=0.005$, exhibit splitting and shifting of the noise peaks under the influence of the transverse H field (for a detailed discussion of transverse magnetic-field effects on the effective shape and areas of the constriction, pertaining to the conductance of wires modeled by a soft-wall confining po-

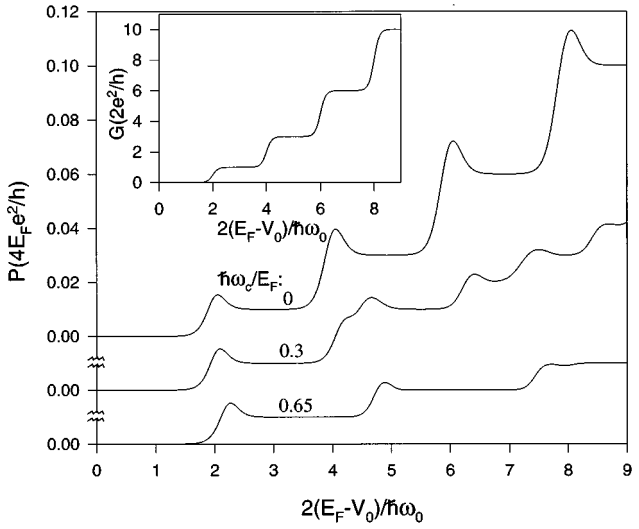

FIG. 8. Noise in a nanowire modeled via a soft-wall potential with $\omega_x=\omega_y=\omega_o$ and $\omega_0/\omega_z=\sqrt{10}$, with $k_BT/E_F=0.005$ and $\mathrm{eV}/E_F=0.05$, plotted vs ξ. Results are shown for different values of an applied transverse magnetic field, specified by $\hbar\omega_c/E_F$, where ω_c is the cyclotron frequency. Note increased splitting and shifting of the shot-noise peaks as the magnetic field is increased. Inset: Conductance (in units of $2e^2/h$) of a cylindrical nanowire ($\omega_x=\omega_y=\omega_0$) modeled via a soft-wall confining potential, for $T=0$, $V\to 0$, and $H=0$, plotted vs $\xi=2\ (E_F-U_0)/\hbar\omega_0$, which is equivalent to the dimensionless parameter k_Fa_0 used in the hard-wall confinement model. The effective length of the wire is given by $\omega_0/\omega_z=\sqrt{10}$. Note the higher degeneracy of the conductance steps (in comparison to that in Fig. 1) corresponding to the harmonic-oscillator spectral degeneracy.

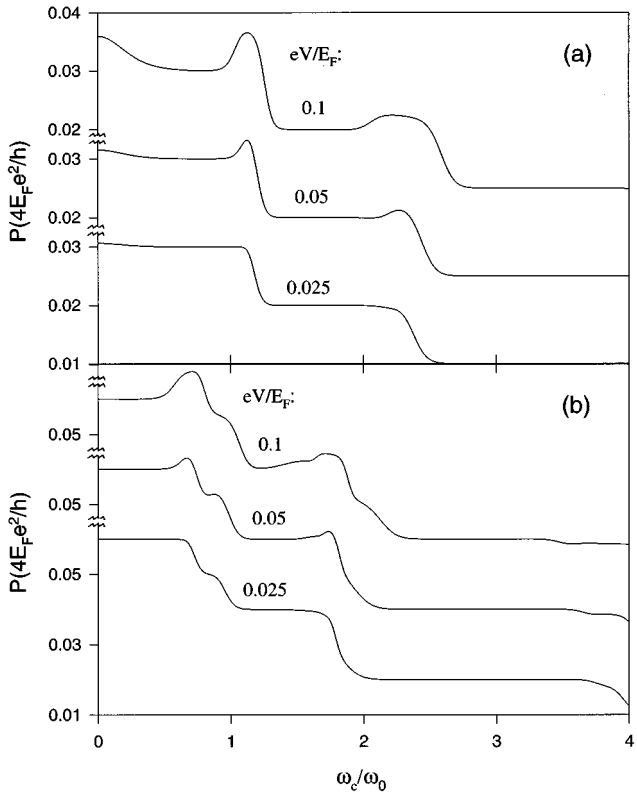

FIG. 9. Noise spectra (in units of $4E_Fe^2/h$) for a nanowire modeled via a soft-wall potential with $\omega_x=\omega_y=\omega_0$ and ω_0/ω_z, plotted vs the magnitude of the applied transverse magnetic field (specified by ω_c/ω_0, where ω_c is the cyclotron frequency). Results are shown for two values of ξ [5.5 and 7.0 shown in (a) and (b), respectively]. In each case results are shown for several values of the applied voltage across the wire (eV/E_F) as denoted.

tential, see Ref. 20). These results are similar to those discussed in Sec. III A for a longitudinal magnetic field.

Noise spectra plotted versus ω_c are shown in Figs. 9(a) and 9(b) for $\xi=5.5$ and 7.0, respectively, for different values of the applied voltage V. For the lowest value of $\mathrm{eV}/E_F=0.025$ we observe transitions between (thermal) noise plateaus associated with magnetic-field-induced switching between quantized conductance plateaus, caused by shifting of the (transverse) electron energy levels by the applied magnetic field. For higher voltage values (see curves for $\mathrm{eV}/E_F=0.05$ and 0.1) the switching is accompanied by quantum-shot-noise peaks.

It is of interest to investigate the influence of the shape of the cross section of the quantum wire on the noise power. In Fig. 10(a) we show the noise spectra versus ω_c for various cross-sectional shapes and orientations with respect to the direction of a transverse magnetic field, plotted for $\xi=7$, $k_BT/E_F=0.005$, and $\mathrm{eV}/E_F=0.1$. In these calculations the cross-sectional area of the constrictions was held constant, i.e., $\omega_x\omega_y=\mathrm{const}$.

The noise power corresponding to the wire having an elliptical cross section with its small axis oriented along the transverse magnetic field exhibits the fastest decrease as a function of ω_c. A similar effect on the conductance of wires [thus pertaining to the thermal noise, see Eq. (2)] has been discussed in Ref. 20. For a wire with a cross-sectional asymmetry $\omega_x/\omega_y=1/3$ shown in Fig. 10(a), the number of current-carrying edge modes is smaller for any given magnetic field than for the configurations with $\omega_x/\omega_y=1$ and 3, and therefore the conductance is smaller for this configuration, resulting in smaller thermal noise contributions.

In Fig. 10(b) we display for $T=0$ shot-noise spectra versus ω_c, corresponding to wires with the same cross-sectional shapes as discussed above. It is easily seen that the shot noise in the wire with the elliptical cross section having its longer axis oriented along the magnetic field is larger than in the wires with other cross-sectional configurations. To explain this phenomenon we consider a magnetic field oriented along the y axis (the z axis corresponds to the axis of symmetry of the wire) with the following gauge chosen for the corresponding vector potential $\mathbf{A}=(zH_y,0,0)$. After diagonalization of the Hamiltonian in a mixed momentum-coordinate representation ($P_x/\omega_x m^*$, y, z; see Ref. 20) we obtain a Hamiltonian, with the potential U taking a form as in Eq. (14), with ω_1, ω_2, and ω_3 replacing ω_x, ω_y, and ω_z, respectively, where

$$\omega_1^2=\tfrac{1}{2}(\omega_x^2-\omega_z^2+\omega_c^2)+\tfrac{1}{2}[\omega_c^4+2\omega_c^2(\omega_x^2-\omega_z^2)+(\omega_x^2+\omega_z^2)^2]^{1/2}, \tag{16a}$$

$$\omega_2^2=\omega_y^2, \tag{16b}$$

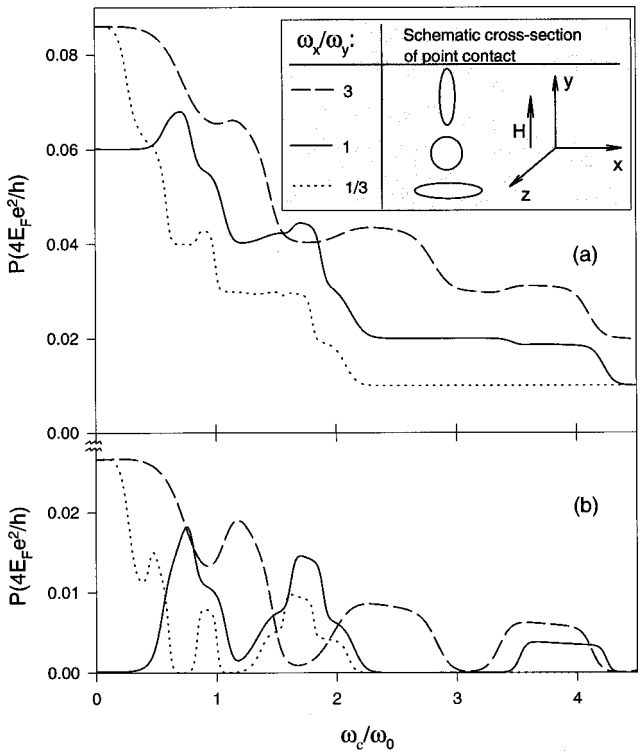

FIG. 10. Noise spectra (in units $4E_F e^2/h$) for a nanowire modeled via a soft-wall potential vs the strength of an applied transverse magnetic field (expressed in terms of $\omega_c/\sqrt{\omega_x\omega_y}$), plotted for various values of ω_x/ω_y, while maintaining a constant value of the cross-sectional area of the constriction, i.e., $\omega_x\omega_y=\omega_0^2=\text{const}$. In the calculations we used $\xi=7$, $\text{eV}/E_F=0.1$, $(\omega_x\omega_y)^{1/2}/\omega_z=\sqrt{10}$. In (a) $k_BT/E_F=0.005$ and in (b) $T=0$. The relative orientations of the cross-sectional axes and the transverse magnetic field are shown in the inset.

$$\omega_3^2=\tfrac{1}{2}(-\omega_x^2+\omega_z^2-\omega_c^2)+\tfrac{1}{2}[\omega_c^4+2\omega_c^2(\omega_x^2-\omega_z^2)+(\omega_x^2+\omega_z^2)^2]^{1/2}. \tag{16c}$$

For the case of a circular cross section, i.e., $\omega_x/\omega_y=1$, the above results transform to those given by Eq. (27) in Ref. 20. Note that the transverse frequency ω_y responsible for the confinement in the direction of the applied transverse magnetic field remains unchanged [Eq. (16b)].

In the weak magnetic-field regime, $\omega_c \ll \omega_x$, we get for ω_1 and ω_3

$$\omega_1 \simeq \omega_x\left(1+\frac{1}{2}\frac{\omega_c^2}{\omega_x^2+\omega_z^2}\right), \tag{17a}$$

$$\omega_3 \simeq \omega_z\left(1-\frac{1}{2}\frac{\omega_c^2}{\omega_x^2+\omega_z^2}\right). \tag{17b}$$

On the other hand, in the strong-field limit, $\omega_c \gg \omega_x$,

$$\omega_1 \simeq \omega_c, \tag{18a}$$

$$\omega_3 \simeq \omega_z\frac{\omega_x}{\omega_c}. \tag{18b}$$

The increase of the transverse frequency ω_1 as a function of the strength of the magnetic field leads to a decrease in the effective cross-sectional area and to depopulation of the subbands (i.e., decrease in the number of conducting channels), resulting in a decrease of the conductance and thermal noise, as described above in conjunction with Fig. 10(a).

The decrease of the frequency ω_3 [see Eqs. (17b) and (18b)] with the strength of the transverse magnetic field corresponds to an effective lengthening of the constriction that leads to a decrease of the shot noise as we already discussed above. It is seen from Eq. (16c) that ω_3 depends only on the magnetic field and on the parameters defining the constriction in the plane normal to the magnetic field, i.e., ω_z and ω_x. From Eqs. (17b) and (18b) we note that for a given transverse magnetic field the effective length of the constriction is larger (i.e., ω_3 is smaller) for smaller values of ω_x (i.e., less confinement in that direction) leading to suppression of the shot noise.

IV. SUMMARY

Noise in mesoscopic and nanoscale systems is of great interest since it (particularly shot noise) provides insights into carrier kinetics with a larger sensitivity to the Pauli principle, carrier interactions, correlations, and quantization conditions, than the conductance (in the limit of zero frequency).[12] Indeed, recent progress in experimental fabrication and measurement techniques allowed measurement of shot noise in 2D mesoscopic systems [Ref. 14, and Fig. 2(b) in Ref. 6].

In this paper we investigated noise spectra of ballistic electron transport in 3D nanowires in field-free conditions, and under the influence of applied magnetic fields, as well as finite voltages. As emphasized by us previously, in the context of studies of magnetic field[16,17,20] and finite voltage[22] effects on quantized conductance and thermopower in nanowires, the ability to modify and control electronic transport in such systems by externally applied fields is of particular interest, since currently used experimental methods for generation and interrogation of 3D nanowires[4] (e.g., tip-based methods, mechanical break junctions, and pin-plate setups) do not readily allow fabrication and measurements of reproducible structures.

We studied here the noise characteristics in adiabatically shaped nanowires, modeled via hard- or soft-wall confining potentials. In both cases we find that the amplitudes of the shot-noise peaks, occurring when the quantized conductance of the wire changes from one conductance plateau to another, are suppressed [see, e.g., Eqs. (9)–(12), and Fig. 2] for effectively longer wires [i.e., for increasing values of the ratio R/a_0 between the axial radius of the wire, R, and the radius of the narrowmost cross section, a_0, see Fig. 1 (inset)]. This reflects enhancement of the time correlation between current-carrying states in longer quantum constrictions.

In a magnetic field (longitudinal or transverse) the shot-noise peaks plotted versus k_Fa_0 undergo splitting and shifting (see, e.g., Fig. 3; for a similar effect in the presence of an applied transverse magnetic field, calculated for a soft-wall confining potential, see Fig. 8). These effects originate from removal of the degeneracies of the conducting modes (trans-

verse energy levels) and shifting of their energies by the applied magnetic field. For a wire with a small number of conducting channels the effect of the magnetic field can lead to most significant variations in the noise spectrum as a function of the field strength (see, e.g., Fig. 4 where for a hard-wall wire with a single conducting channel magnetic-field-induced ''shot-noise blockade'' is shown, i.e., observe the curve corresponding to $k_F a_0 = 2.5$). Furthermore, control of the noise spectrum through applied finite voltages in field-free conditions and under the influence of a magnetic field have been demonstrated (see, e.g., Figs. 5 and 6 for a hard-wall wire and a longitudinal magnetic field, and Fig. 9 for a soft-wall wire and a transverse magnetic field).

We also find that in a transverse magnetic field the cross-sectional shape of the nanowire may influence the noise spectra due to different contributions from the current-carrying edge states depending on the azimuthal orientation of the applied field (e.g., compare the noise spectra for elliptically shaped cross sections shown in Fig. 10). This suggests that cross-sectional shape anisotropy of nanowires could be detected through analysis of the noise spectra as a function of the azimuthal direction of applied transverse magnetic fields.

Finally, we remark that while the theoretical results presented in this paper are general, experimental observations of the predicted magnetic-field effects on the noise spectra of nanowires (as well as on the conductance as described in Ref. 17) may be most readily obtained for semimetallic nanowires due to the reduced electron concentrations (i.e., small k_F values), and consequently the relatively large cross-sectional wire radii corresponding to a small number of conducting channels. For example, in bismuth wires $k_F \approx 2\times10^6$ cm^{-1}, and a single conducting channel ($k_F a_0 \approx 3$; see Fig. 1) corresponds to $a_0 \sim 1.5\times10^{-6}$ cm. Thus the magnetic field required to create a magnetic-flux quantum in such a wire is about $H = \varphi_0/\pi a_0^2 \sim 10$ T, which is readily accessible experimentally (obviously even smaller fields are required for wider nanowires corresponding to larger conductance values).

ACKNOWLEDGEMENTS

We thank R. Landauer for his comments on the manuscript. This research was supported by the U.S. Department of Energy, Grant No. FG05-86ER45234. Calculations were performed at the Georgia Tech Center for Computational Materials Science.

[1] H. van Houten, C. W. J. Beenakker, and B. J. van Wees, Semicond. Semimet. **35**, 9 (1992).
[2] E. N. Bogachek, A. M. Zagoskin, and I. O. Kulik, Fiz. Nizk. Temp. **16**, 1404 (1990) [Sov. J. Low Temp. Phys. **16**, 796 (1990)].
[3] U. Landman, W. D. Luedtke, N. A. Burnham, and R. J. Colton, Science **248**, 454 (1990).
[4] See papers in *Nanowires*, edited by P. A. Serena and N. Garcia (Kluwer, Dordrecht, 1997).
[5] Sh. Kogan, *Electronic Noise and Fluctuations in Solids* (Cambridge University Press, Cambridge, 1996).
[6] M. J. M. de Jong and C. W. J. Beenakker, in *Mesoscopic Electron Transport*, edited by L. L. Sohn, L. P. Kouwenhoven, and G. Schon (Kluwer, Dordrecht, 1997), p. 225.
[7] I. O. Kulik and A. N. Omelyanchuk, Fiz. Nizk. Temp. **10**, 305 (1984) [Sov. J. Low Temp. Phys. **10**, 158 (1984)].
[8] Yu. V. Sharvin, Zh. Eksp. Teor. Fiz. **48**, 984 (1965) [Sov. Phys. JETP **21**, 655 (1965)].
[9] R. Landauer, Philos. Mag. **21**, 863 (1970).
[10] V. A. Khlus, Zh. Eksp. Teor. Fiz. **93**, 2179 (1987) [Sov. Phys. JETP **66**, 1243 (1987)].
[11] G. B. Lesovik, Pis'ma Zh. Eksp. Teor. Fiz. **49**, 513 (1989) [JETP Lett. **49**, 592 (1989)].
[12] R. Landauer, Physica D **38**, 226 (1989); R. Landauer and Th. Martin, Physica B **175**, 167 (1991); R. Landauer, *ibid.* **227**, 156 (1996).
[13] M. Buttiker, Phys. Rev. Lett. **65**, 2901 (1990); Phys. Rev. B **46**, 12 485 (1992).
[14] M. Reznikov, M. Heiblum, H. Shtrikman, and D. Mahalu, Phys. Rev. Lett. **75**, 3340 (1995); A. Kumar, L. Saminadayar, D. C. Glattli, Y. Jin, and B. Etienne, *ibid.* **76**, 2778 (1996).
[15] L. I. Glazman, G. B. Lesovik, D. E. Khmelnitskii, and R. I. Shekhter, Pis'ma Zh. Eksp. Teor. Fiz. **48**, 218 (1988) [JETP Lett. **48**, 238 (1988)].
[16] E. N. Bogachek, A. G. Scherbakov, and U. Landman, Phys. Rev. B **54**, R11 094 (1996).
[17] E. N. Bogachek, A. G. Scherbakov, and U. Landman, Phys. Rev. B **53**, R13 246 (1996).
[18] E. N. Bogachek, A. G. Scherbakov, and U. Landman, Phys. Rev. B **56**, 1065 (1997).
[19] L. Y. Chen and S. C. Ying, Mod. Phys. Lett. B **9**, 573 (1995).
[20] A. G. Scherbakov, E. N. Bogachek, and U. Landman, Phys. Rev. B **53**, 4054 (1996).
[21] M. Buttiker, Phys. Rev. B **41**, 7906 (1990).
[22] E. N. Bogachek, A. G. Scherbakov, and U. Landman, Phys. Rev. B **56**, 14 917 (1997).